Title

Specific Macronutrients Exert Unique Influences on the Adipose-Liver Axis to Promote Hepatic Steatosis in Mice

Journal

Cellular and Molecular Gastroenterology and Hepatology, 4(2)

ISSN

2352-345X

Authors

Duwaerts, Caroline C
Amin, Amin M
Siao, Kevin
et al.

Publication Date

2017-09-01

DOI

10.1016/j.jcmgh.2017.04.004

Peer reviewed

cmgh
CELLULAR AND MOLECULAR GASTROENTEROLOGY AND HEPATOLOGY

ORIGINAL RESEARCH

Specific Macronutrients Exert Unique Influences on the Adipose-Liver Axis to Promote Hepatic Steatosis in Mice

Caroline C. Duwaerts,[1,2] Amin M. Amin,[1,2] Kevin Siao,[1,2] Chris Her,[1,2] Mark Fitch,[3] Carine Beysen,[4] Scott M. Turner,[4] Amanda Goodsell,[1,2] Jody L. Baron,[1,2] James P. Grenert,[2,5] Soo-Jin Cho,[5] and Jacquelyn J. Maher[1,2]

[1]Department of Medicine, University of California, San Francisco, California; [2]The Liver Center, University of California, San Francisco, California; [3]Department of Nutritional Sciences and Toxicology, University of California, Berkeley, California; [4]KineMed, Inc, Emeryville, California; and [5]Department of Pathology, University of California, San Francisco, California

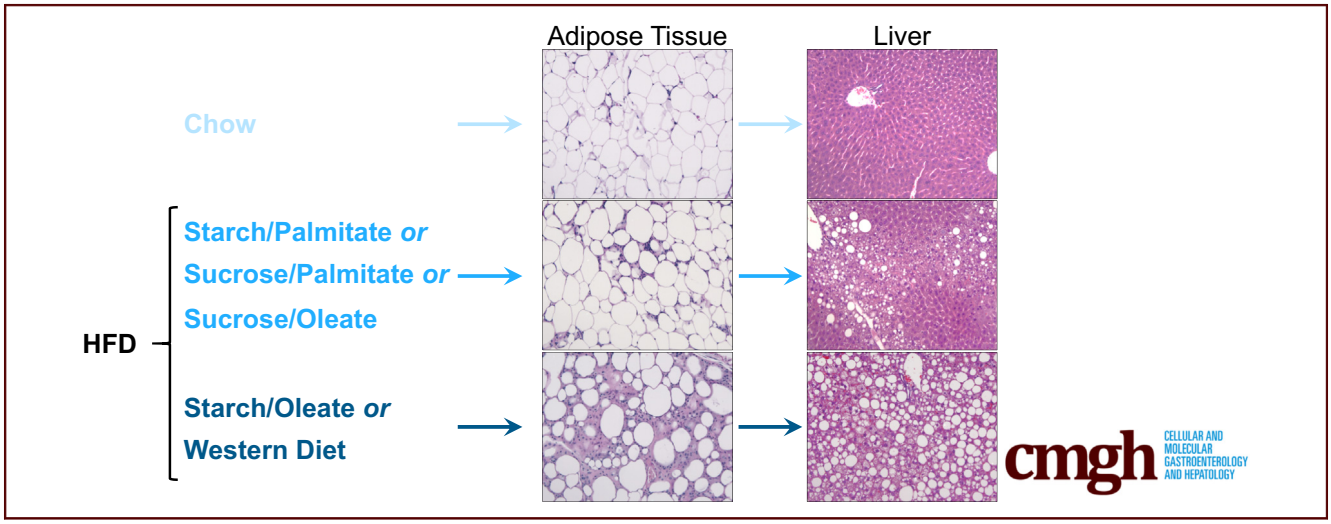

SUMMARY

Testing the effect of specific macronutrient combinations on mouse metabolism in vivo, the authors determined that diets pairing starch as carbohydrate with oleate as fat (42%:42% kcal) induced significant white adipose tissue pathology and hepatic steatosis compared with other isocaloric combinations.

BACKGROUND & AIMS: The factors that distinguish metabolically healthy obesity from metabolically unhealthy obesity are not well understood. Diet has been implicated as a determinant of the unhealthy obesity phenotype, but which aspects of the diet induce dysmetabolism are unknown. The goal of this study was to investigate whether specific macronutrients or macronutrient combinations provoke dysmetabolism in the context of isocaloric, high-energy diets.

METHODS: Mice were fed 4 high-energy diets identical in calorie and nutrient content but different in nutrient composition for 3 weeks to 6 months. The test diets contained 42% carbohydrate (sucrose or starch) and 42% fat (oleate or palmitate). Weight and glucose tolerance were monitored; blood and tissues were collected for histology, gene expression, and immunophenotyping.

RESULTS: Mice gained weight on all 4 test diets but differed significantly in other metabolic outcomes. Animals fed the starch-oleate diet developed more severe hepatic steatosis than those on other formulas. Stable isotope incorporation showed that the excess hepatic steatosis in starch-oleate–fed mice derived from exaggerated adipose tissue lipolysis. In these mice, adipose tissue lipolysis coincided with adipocyte necrosis and inflammation. Notably, the liver and adipose tissue abnormalities provoked by starch-oleate feeding were reproduced when mice were fed a mixed-nutrient Western diet with 42% carbohydrate and 42% fat.

CONCLUSIONS: The macronutrient composition of the diet exerts a significant influence on metabolic outcome, independent of calories and nutrient proportions. Starch-oleate appears to cause hepatic steatosis by inducing progressive adipose tissue injury. Starch-oleate phenocopies the effect of a Western diet; consequently, it may provide clues to the mechanism whereby specific nutrients cause metabolically unhealthy obesity. *(Cell Mol Gastroenterol Hepatol 2017;4:223–236; http://dx.doi.org/10.1016/j.jcmgh.2017.04.004)*

Keywords: Steatohepatitis; Oleate; Starch; Adipose Tissue.

See editorial on page 301.

Obesity affects nearly 38% of adults in the United States and more than 10% of adults worldwide.[1,2] Although obesity is often accompanied by dysmetabolism and inflammation in the form of insulin resistance, type 2 diabetes, hypertension, and cardiovascular disease, not all obese individuals display these comorbidities. Experts now separate obese persons into 2 categories based on the presence or absence of metabolic derangements: the metabolically healthy obese (MHO) and the metabolically unhealthy obese (MUO). The stringency by which metabolic "health" is defined is not yet completely standardized. Accordingly, somewhere between 10% and 50% of obese individuals are classified as MHO, whereas the remainder are considered MUO.[3]

Hepatic steatosis is an important feature of the MUO phenotype.[4] Scientists have recently reported that hepatic steatosis predates other features of dysmetabolism in obesity,[5] suggesting it is a predictor of more advanced metabolic disease. Given the importance of hepatic steatosis to the definition and possibly the pathogenesis of MUO, there is great interest in defining the factors that promote metabolic deterioration in the obese. One variable that has been scrutinized as a possible determinant of MUO is diet. Although some large population studies have identified subtle differences in diet as a determinant of the MUO phenotype,[6,7] others have not been able to detect a difference in either calorie or nutrient consumption between MHO and MUO subgroups.[8–10] This may be due to the imperfect quality of dietary data in population studies, which in general rely on self-report and recall.

Despite the paucity of epidemiologic evidence that diet is a risk factor for MUO, carefully controlled intervention studies argue that manipulation of individual nutrients can impact metainflammation.[11–13] Still, it is uncertain whether specific carbohydrate (CHO)-fat combinations, when tested within the context of calorically matched diets, have unique effects on metabolic health over the long term.[14,15] The goal of this study was to determine whether diets similar in nutrient content to the typical American diet, but differing in their sources of CHO and fat, exert different effects on the livers of mice. The results indicate that 4 different dietary formulas, matched in calories, CHO, and fat content but with different macronutrient composition, did indeed induce significantly different degrees of hepatic steatosis over 6 months. The 4 formulas also induced significantly different degrees of adipose tissue injury and inflammation, and demonstrated a striking direct relationship between adipose tissue damage and hepatic lipid accumulation. Surprisingly, the single macronutrient that promoted the worst metabolic phenotype in mice was oleate, a monounsaturated fat.

Methods

Animals and Diets

Adult male mice (C57BL/6J and C3H/HeOuJ, The Jackson Laboratory, Bar Harbor, ME) were used for all studies. Some were fed standard laboratory chow as a control diet (PicoLab Diet # 5053, St. Louis, MO). Others were randomly assigned to 1 of 4 isocaloric high-energy diets comprising 15% kcal protein, 42% kcal CHO, and 42% kcal fat (Dyets, Inc, Bethlehem, PA) (Table 1). The groups were named for their primary ingredients: starch-palmitate, sucrose-palmitate, starch-oleate, and sucrose-oleate. A separate group of mice was fed a Western diet (TD.88137, Envigo Teklad, Madison, WI) comprising 42% kcal CHO and 42% kcal fat of mixed sources. Animals were group-housed with ad libitum access to food and water and were treated in accordance with Institutional Animal Care and Use Committee guidelines at the University of California, San Francisco.

Serum Chemistries

Serum alanine aminotransferase was measured on an ADVIA 1800 autoanalyzer (Siemens Healthcare Diagnostics, Deerfield, IL) in the clinical chemistry laboratory at the Zuckerberg San Francisco General Hospital.

Glucose Tolerance Test

Glucose tolerance tests were performed 1 week prior to the end of each dietary study as previously described.[16]

Measurement of Hepatic Lipids

Lipids were extracted from liver tissue employing the Folch method.[17] Liver triglyceride (TG) was quantified biochemically as described previously.[18]

Histology and Immunohistochemistry

Sections of liver and epididymal white adipose tissue (eWAT) were stained with H&E and blindly scored by a pathologist (J.P.G., liver; S.J.C., adipose tissue). Liver sections were scored for steatosis, ballooning, and inflammation using the criteria developed by Kleiner et al.[19] Adipose tissue was scored for necrosis on a 0 to 3 scale as follows: 0 = scattered crown-like structures only, 1 = focal areas of necrosis affecting <5% of the total tissue, 2 = 5%–25% necrosis, 3 = >25% necrosis. Adipose tissue necrosis is defined as anuclear or disintegrated adipocytes, of varying size, surrounded by aggregates of inflammatory cells with or without multinucleate giant cells present.[20] Additional sections of eWAT were subjected to immunohistochemistry for perilipin 1 (#9349, Cell Signaling Technology, Danvers, MA) and NKp46 (#137615, Biolegend, San Diego, CA).

Abbreviations used in this paper: **CHO, carbohydrate; DNL, de novo lipogenesis; eWAT, epididymal white adipose tissue; MHO, metabolically healthy obese; MUO, metabolically unhealthy obese; NK, natural killer; TG, triglyceride.**

Most current article

2352-345X
http://dx.doi.org/10.1016/j.jcmgh.2017.04.004

Table 1. Dietary Composition

	Nutrient (*g/kg*)	Chow	Sucrose palmitate	Starch palmitate	Sucrose oleate	Starch oleate	Western diet
Amino acids	L-Alanine	11.9	4.5	4.5	4.5	4.5	5.1
	L-Arginine, fb	12.9	6.3	6.3	6.3	6.3	6.4
	L-Aspartic acid	21.9	11.3	11.3	11.3	11.3	11.7
	L-Cystine	3.6	3.7	3.7	3.7	3.7	0.5
	L-Glutamic acid	41.8	36.2	36.2	36.2	36.2	35.5
	Glycine	9.7	3.1	3.1	3.1	3.1	3.1
	L-Histidine, f b	5.3	4.5	4.5	4.5	4.5	4.9
	L-Isoleucine	8.6	8.4	8.4	8.4	8.4	9.8
	L-Leucine	15.7	15.3	15.3	15.3	15.3	15.6
	L-Lysine-HCl	11.8	16.1	16.1	16.1	16.1	13.7
	L-Methionine	6.2	2.0	2.0	2.0	2.0	10.5
	L-Phenylalanine	9.1	8.7	8.7	8.7	8.7	8.6
	L-Proline	13.1	20.4	20.4	20.4	20.4	17.6
	L-Serine	9.8	9.4	9.4	9.4	9.4	9.8
	L-Threonine	7.8	6.6	6.6	6.6	6.6	7.4
	L-Tryptophan	2.4	2.1	2.1	2.1	2.1	2.0
	L-Tyrosine	6.0	9.2	9.2	9.2	9.2	9.0
	L-Valine	9.7	9.9	9.9	9.9	9.9	11.7
	Choline chloride	2.0	2.0	2.0	2.0	2.0	2.0
	SUBTOTAL	209.3	179.7	179.7	179.7	179.7	184.9
Carbohydrate	Cornstarch	286	—	472.9	—	472.9	150.0
	Cellulose	216[a]	80.0	80.0	80.0	80.0	50.0
	Fructose	2.4	—	—	—	—	—
	Glucose	1.9	—	—	—	—	—
	Lactose	13.4	—	—	—	—	—
	Sucrose	32.4	456.9	—	456.9	—	341.5
	SUBTOTAL	552.1	536.9	552.9	536.9	552.9	541.5
Fat	Saturated fats	7.8	220.6	205.4	19.4	18.1	131.0
	Monounsaturated fats	9.7	1.4	1.3	187.1	174.2	57.9
	Polyunsaturated fats	32.5	9.0	8.4	24.5	22.8	21.6
	Cholesterol	0.1	—	—	—	—	1.5
	Main source	Soybean oil	Tripalmitin[b]	Tripalmitin[b]	High-oleic sunflower oil	High-oleic sunflower oil	Anhydrous milk fat
	SUBTOTAL	50.1	231.0	215.1	231.0	215.0	212.0
% kcal	Protein	24.5	14.6	15.4	14.6	15.4	15.2
	CHO	62.3	42.7	42.5	42.7	42.5	42.7
	Fat	13.1	42.7	42.1	42.7	42.1	42.0

[a]Undefined fiber.
[b]Tripalmitin diets were enriched with safflower oil for essential fatty acid supplementation (reflected in totals).

Measurement of Adipose Tissue Gene Expression

Adipose tissue RNA was isolated using an RNeasy lipid tissue kit (Qiagen, Germantown, MD). eWAT gene expression was analyzed using an nCounter mouse immunology gene expression codeset from NanoString Technologies (XT_PGX_MmV1_Immunology_KIT, Seattle, WA). The assay was performed by the Stanford Functional Genome Facility and data were analyzed using nSolver 2.5 software (NanoString Technologies).

Measurement of De Novo Lipogenesis

De novo lipogenesis (DNL) in liver and adipose tissue was measured by the use of ^2H_2O labeling combined with mass isotopomer distribution analysis as described previously.[21,22] For experiments assessing hepatic DNL, animals received an intraperitoneal bolus of saline prepared with 99% ^2H_2O (30 mL/kg) 1 day prior to killing and were placed on drinking water containing 8% ^2H_2O for 24 h. For experiments assessing adipose tissue DNL, different mice received a comparable loading dose of ^2H_2O-saline 1 week prior to euthanasia and were maintained on 8% ^2H_2O in the drinking water for 7 days. Labeling periods were longer for adipose tissue to ensure adequate isotope enrichment of cellular lipids.[23] ^2H_2O incorporation into hepatic or adipose tissue palmitate was assessed by mass spectrometry and mass isotopomer distribution analysis calculations were based on 22 possible sites for deuterium incorporation.

Adipose Tissue Lipolysis

eWAT was collected from mice fed experimental diets for 6 weeks. Tissue fragments (20 to 40 mg) were washed with cold phosphate-buffered saline and cultured in Dulbecco's modified Eagle medium for 1 to 19 hours at 37°C, with or without forskolin (10 mM). The amount of free fatty acid released into the medium was quantitated (LIP-1-NC, Zenbio, Research Triangle Park, NC) and normalized per gram of tissue.

Stromal Vascular Cell Isolation and Flow Cytometry

eWAT was collected and stromal vascular cells were isolated by collagenase digestion. Briefly, fat pads were incubated with 0.2 mg/mL collagenase NB8 (Crescent Chemical Co, Islandia, NY) for 60 minutes at 37°C and the cell suspension serially filtered through 100-mm, 70-mm, and 40-mm cell strainers. After centrifugation at 500 g for 5 minutes, cells were stained for flow cytometry with the following antibodies from Biolegend: PerCP-Cy5.5-CD11b (#101228), APC/FIRE-CD45 (#103154), AF700-Ly-6C (#128024), FITC-NKp46 (#137606), and APC-TCRβ (#109212).

Statistical Analysis

All experimental results were compared using 1-way analysis of variance followed by a Tukey post hoc test, unless otherwise noted in the figure legends. Statistical analyses were performed with Prism 6 software (GraphPad, La Jolla, CA).

Data

All authors had access to the study data and have reviewed and approved the final manuscript.

Results

A Starch-Oleate Diet Induces More Hepatic Steatosis Than Do Isocaloric Diets Featuring Other Nutrients

Mice were fed isocaloric high-energy diets, identical in nutrient content (42:42:15 CHO:fat:protein) but differing in macronutrient composition, for 6 months. Initial studies conducted with 2 strains of mice (C3H and C57BL/6) revealed that C3H mice developed hepatic steatosis rapidly in response to high-energy feeding (Figure 1), and thus this strain was used for all subsequent experiments. All mice consumed similar amounts of food over the study period and all mice on high-energy diets gained more weight than chow control mice (Figure 2*A* and *B*). Despite this, only mice fed starch-enriched diets displayed hyperinsulinemia at 6 months (Table 2), and only those fed starch-oleate exhibited glucose intolerance (Figure 1*C*). All mice fed high-energy diets developed hepatic steatosis compared to chow control mice. The degree of steatosis, however, differed among the 4 experimental groups. Mice fed starch-oleate displayed the worst steatosis, accumulating at least 40% more hepatic lipid than the other 3 high-energy diet groups (Figure 2*D* and *E*). Starch-oleate–fed mice also showed more evidence of liver injury than did mice in the other high-energy groups. They displayed the most hepatocyte ballooning and had the highest alanine aminotransferase levels of all groups under study (Table 2); however, no group demonstrated significant fibrosis by Sirius red staining (data not shown).

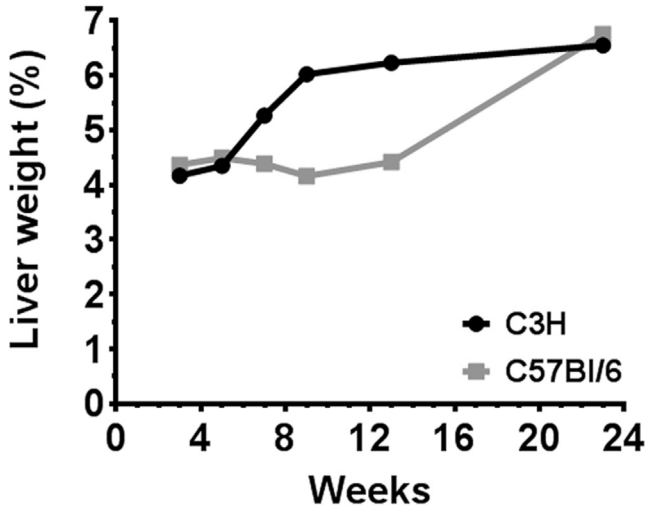

Figure 1. Strain-dependent difference in the hepatic response to high-energy feeding. C3H and C57BL/6 mice were fed a high-energy diet for various intervals up to 6 months. Graph illustrates liver weight as a percent of body weight at each interval. Values represent means for n = 2 to 4.

Starch-Oleate Feeding Increases Hepatic DNL and Incorporation of Fat From Adipose Tissue

To determine whether hepatic steatosis in starch-oleate–fed mice was due to a disproportionate increase in hepatic DNL, we measured DNL directly by deuterium incorporation into liver palmitate. DNL was elevated in all mice fed the experimental diets compared to chow, but there was no difference among the 4 high-energy groups (Figure 3*A*). Instead, the bulk of the palmitate in starch-oleate–fed livers derived from sources other than DNL (Figure 3*B*). The other (unlabeled) sources represented in Figure 3*B* include dietary fat and fatty acids from adipose tissue lipolysis. Because the starch-oleate diet contained little or no palmitate, the large amount of palmitate in starch-oleate livers likely derived from adipose tissue lipolysis.

Because our data suggested adipose tissue lipolysis was more prominent in mice fed starch-oleate than in other high-energy diets, we investigated the effect of each diet on eWAT, the main visceral fat depot in mice. In chow-fed control mice, eWAT weight measured as a percentage of body weight increased significantly between 3 weeks and 6 months (Figure 3*C*). In contrast, eWAT weight percent did not increase in any of the mice fed high-energy diets; in fact, eWAT weight percent declined in mice fed oleate-enriched diets, even dropping below 1% in mice fed starch-oleate for 6 months. At the 6-month interval, an inverse relationship was noted between eWAT weight and liver weight in mice from all dietary groups (Figure 3*D*). Viewing these results together with the stable isotope incorporation data, it is evident that DNL and adipose tissue lipolysis both contribute to hepatic steatosis in response to high-energy diets but adipose tissue lipolysis is disproportionately increased in response to a starch-oleate diet.

Starch-Oleate Feeding Induces Histologic and Functional Changes in eWAT as It Induces Hepatic Steatosis

Diet-induced obesity is known to cause adipose tissue necrosis and inflammation. Because starch-oleate feeding

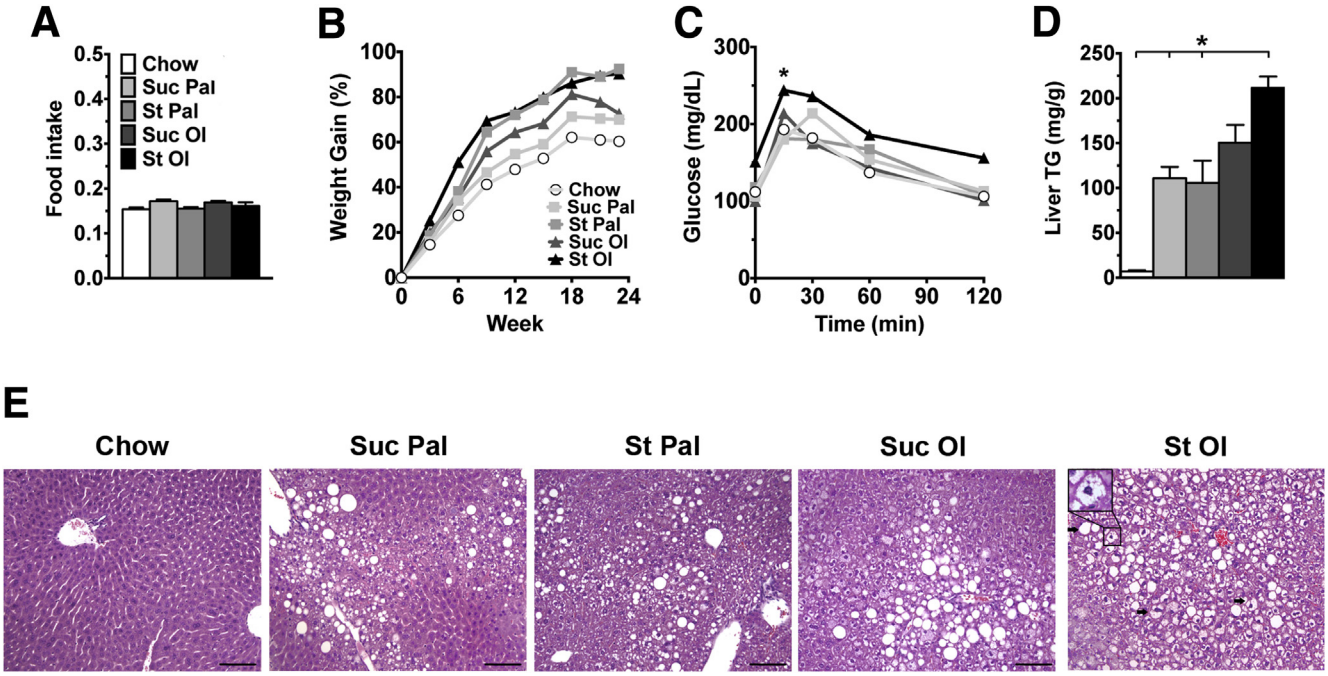

Figure 2. Metabolic and histological features of mice fed chow or custom high-energy diets for 6 months. (*A*) Average food intake, reported as g food consumed per gram of body weight per day, measured biweekly over 6 months. (*B*) Percent body weight gain over time. (*C*) Blood glucose levels following administration of 1.5 g/kg glucose intraperitoneally, performed after 6 months on diet. (*D*) Liver TG in milligrams per gram of liver. (*E*) H&E-stained liver tissue was viewed on a Nikon Microphot FXA microscope (Nikon, Tokyo, Japan) under a 10× objective and photographed using a Spot camera (Spot Imaging, Sterling Heights, MI). Images were compiled in Photoshop CS6 (Adobe Systems Inc, San Jose, CA). Bar = 100 mm. *Arrows* document ballooned hepatocytes. *Inset* highlights a ballooned cell at 40× magnification. Values represent mean ± SE for n = 10, performed as replicate experiments of n = 5 each. *$P < .05$ versus other groups at the same time point. St Ol, starch-oleate; St Pal, starch-palmitate; Suc Ol, sucrose-oleate; Suc Pal, sucrose-palmitate.

caused an unusual loss of eWAT weight percent at 6 months, we elected to explore the kinetics of eWAT atrophy in mice fed this diet over 24 weeks. eWAT mass expanded slightly during the first 5 weeks of feeding, but then began to decline and continued a progressive downward trend through week 24 (Figure 3*E*). Interestingly, liver mass rose slightly during the first 5 weeks of feeding and then rose progressively through week 24 in reciprocal fashion to the adipose tissue. Photomicrographs of the tissues over the time course revealed pronounced infiltration of the eWAT with inflammatory cells as hepatic steatosis progressed (Figure 3*F*). Reviewing adipose tissue histology in mice on all high-energy diets at 6 months, all groups demonstrated at least some adipocyte condensation and formation of crown-like structures, but by far the worst inflammation was present in the starch-oleate group. Inflammatory cell infiltration was accompanied by a loss of perilipin 1 staining indicative of adipocyte necrosis (Figure 4).[24] Formal histology scoring confirmed that starch-oleate–fed mice had significantly more adipose tissue necrosis than did all other groups (Table 3).

To assess adipose tissue function, we measured DNL and lipolysis in adipose tissue from mice fed chow and experimental diets. DNL was significantly reduced in mice fed

Table 2. Liver Histological Scores and Serum Values

	Steatosis (0–3)	Ballooning (0–3)	Inflammation (0–2)	ALT (*IU/L*)	Insulin (*ng/mL*)
Chow	0.0 ± 0.0	0.0 ± 0.0	0.0 ± 0.1	47 ± 3	0.52 ± 0.08
Suc Pal	1.0 ± 0.3	0.0 ± 0.1	0.0 ± 0.1	61 ± 4	0.68 ± 0.13
St Pal	1.0 ± 0.2	0.0 ± 0.2	0.0 ± 0.0	68 ± 4[a]	1.78 ± 0.24[a]
Suc Ol	1.0 ± 0.2	1.0 ± 0.3	0.0 ± 0.1	58 ± 5	0.87 ± 0.37
St Ol	3.0 ± 0.2[b]	2.0 ± 0.2[b]	0.0 ± 0.2	77 ± 4[a]	1.83 ± 1.2[a]

IU, international units; St Ol, starch-oleate; St Pal, starch-palmitate; Suc Ol, sucrose-oleate; Suc Pal, sucrose-palmitate.
[a]$P < .05$ versus chow.
[b]$P < .05$ versus all other groups.

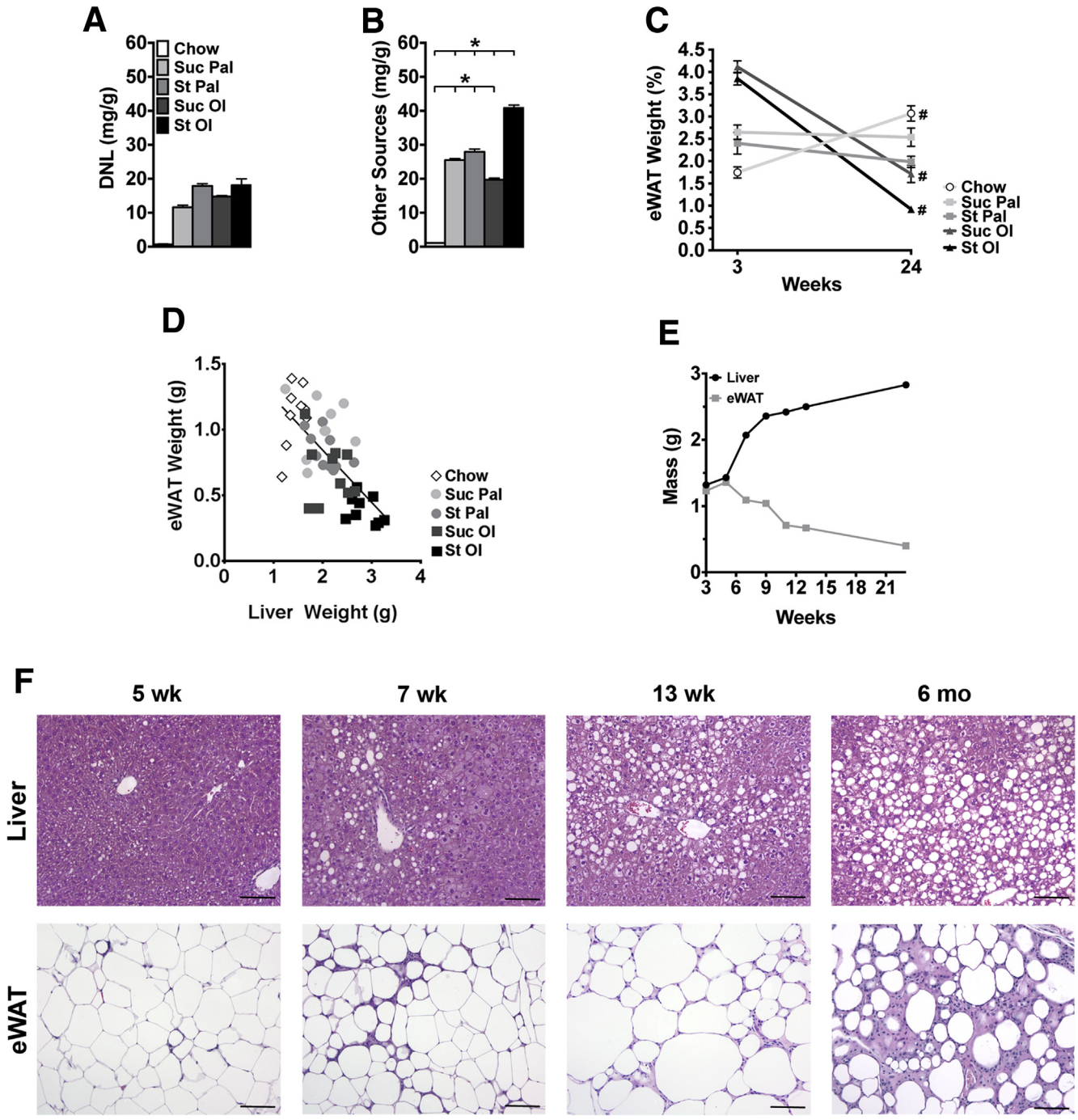

Figure 3. Sources of hepatic lipid at 6 months and changes in eWAT and liver over time in mice fed chow or custom high-energy diets. (*A, B*) Hepatic lipid arising from DNL or other sources measured by stable isotope incorporation. Values represent mean ± SE for n = 10, performed as replicate experiments of n = 5 each. (*C*) eWAT weight as a percent of body weight at 3 weeks (wk) and 24 wk following chow or custom diet feeding. Values represent mean ± SE for n = 10, performed as replicate experiments of n = 5 each. (*D*) Whole liver and total epididymal fat pads (eWAT) were weighed at 6 months (mo). Liver weight was plotted against eWAT weight, and a linear correlation was drawn. Values represent each individual animal, n = 10 per diet group. (*E*) Time course of changes in liver and eWAT weight in starch-oleate–fed mice over 24 weeks. Values represent means of n = 2 at 6 to 13 wk and n = 10 at 3 wk and 24 wk. (*F*) H&E-stained liver and eWAT tissue sections were viewed on a Nikon Microphot FXA microscope under a 10× objective and photographed using a Spot camera. Images were compiled in Photoshop CS6 (Adobe Systems Inc, San Jose, CA). Bar = 100 mm. $^{*}P < .05$; $^{\#}P < .05$ for 3 weeks versus 24 wk of the same diet. St Ol, starch-oleate; St Pal, starch-palmitate; Suc Ol, sucrose-oleate; Suc Pal, sucrose-palmitate.

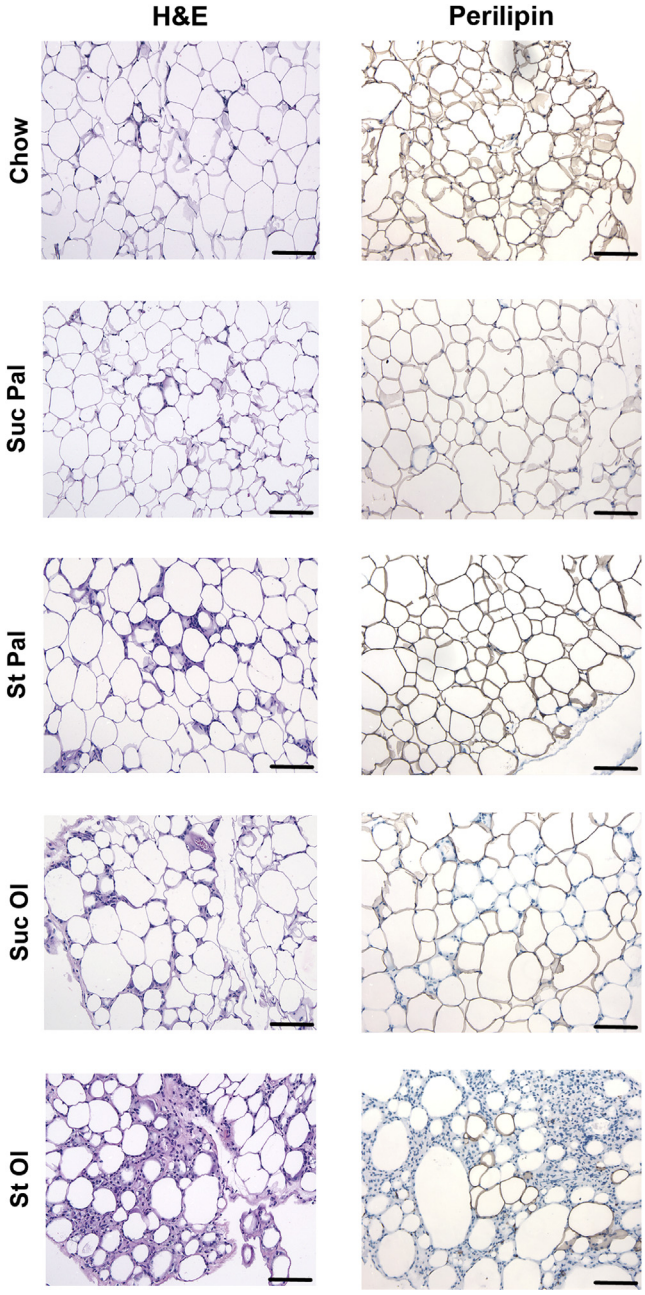

Figure 4. eWAT histology in mice fed chow or custom high-energy diets for 6 months. Adipose tissue sections were stained with H&E or an antibody against perilipin 1. Sections were viewed on a Nikon Microphot FXA microscope under a 10× objective and photographed using a Spot camera. Images were compiled in Photoshop CS6 (Adobe Systems Inc, San Jose, CA). Loss of perilipin 1 (*brown*) staining in adipocyte membranes is indicative of cell death. Bar = 100 mm. St Ol, starch-oleate; St Pal, starch-palmitate; Suc Ol, sucrose-oleate; Suc Pal, sucrose-palmitate.

oleate-enriched diets and particularly starch-oleate, signaling an impairment in fat synthesis and storage (Figure 5*A*). Adipose tissue lipolysis was similar in all dietary groups except mice fed starch-oleate, where it was increased 2-fold (Figure 5*B*). The net effect of reduced DNL and enhanced lipolysis in starch-oleate–fed mice would be a loss of adipose tissue mass, as was observed in vivo (Figure 3*C* and *E*).

Table 3. Epididymal Adipose Tissue Histological Scores

	eWAT Necrosis (0–3)
Chow	0.9 ± 0.2
Suc Pal	0.8 ± 0.3
St Pal	1.2 ± 0.2
Suc Ol	1.1 ± 0.2
St Ol	2.0 ± 0.2[a]

St Ol, starch-oleate; St Pal, starch-palmitate; Suc Ol, sucrose-oleate; Suc Pal, sucrose-palmitate.
[a]$P < .05$ versus all other groups.

To characterize the inflammatory state of adipose tissue from mice fed experimental diets, we performed transcriptomic profiling using an inflammatory gene array. Gene expression clustered by diet, with the groups fed oleate exhibiting the most pronounced proinflammatory profile (Figure 6*A*). Several genes up-regulated by starch-oleate feeding were suggestive of tissue infiltration by macrophages, natural killer (NK) cells and lymphocytes (Figure 6*B*). One of the most strongly up-regulated genes was *KLRA8*, a marker of NK cells.[25] Immunohistochemical staining confirmed that cells expressing the NK marker NKp46 were more abundant in adipose tissue from starch-oleate–fed mice than in tissue from mice fed other diets (Figure 6*C*). Knowing that adipose tissue dysfunction begins early in response to high-energy feeding (Figure 3*E*), we harvested adipose tissue from mice fed high-energy diets for 6 weeks and extracted stromal vascular cells for immunophenotyping by flow cytometry eWAT (Figure 7). Mice fed starch-oleate had 5 times more CD45+ cells than did chow control mice (58,802 ± 5,418 vs 11,447 ± 4,245; $P < .001$); they included NK cells, NK^+T^+ cells, and T cells, as well as resident and inflammatory macrophages (Figure 7). Mice fed oleate with sucrose also displayed an increase in adipose tissue NK cells, but exhibited no change in any other immune cell populations.

Effects of Starch-Oleate Feeding on Liver and Adipose Tissue Phenocopy Those of the Western Diet

The highly defined diets used in this study differ from mixed-nutrient diets commonly linked to obesity and fatty liver disease. To determine whether the effects we observed in response to starch-oleate are generalizable to other formulas, we examined liver and adipose tissue from mice fed a commercial Western diet for 6 months. Mice fed the Western diet closely resembled those fed starch-oleate in both liver and adipose tissue pathology. Similar to starch-oleate–fed mice, Western diet–fed mice developed significant hepatic steatosis at 6 months (Figure 8*A* and *B*). Similar to starch-oleate mice, hepatic lipid in Western diet–fed mice derived in part from DNL, but mostly from other sources (Figure 8*C*). Western diet–fed mice also displayed

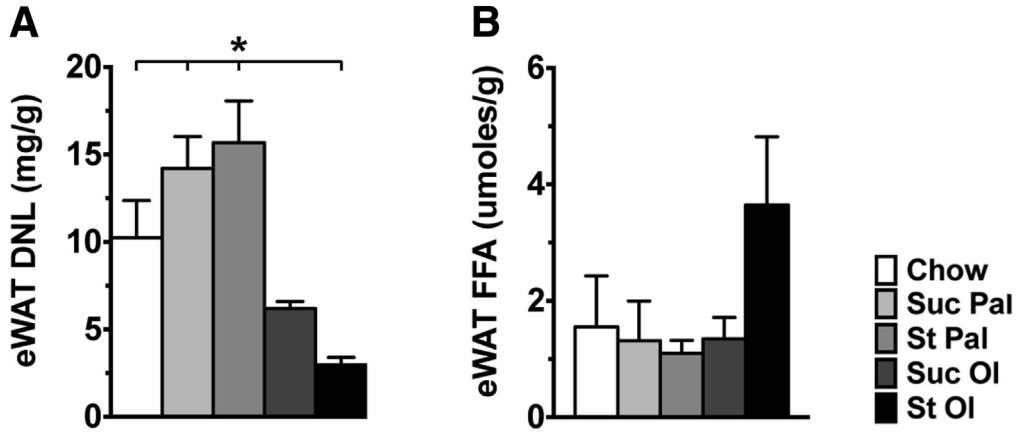

Figure 5. DNL and lipolysis in eWAT from mice fed chow or custom high-energy diets for 6 weeks. (*A*) DNL measured in adipose tissue by stable isotope incorporation over 1 week. (*B*) Basal lipolysis measured ex vivo in eWAT harvested from mice. Forskolin-stimulated lipolysis was similar in all groups (not shown). Values represent mean ± SE for n = 10, performed as replicate experiments of n = 5 each. *$P < .05$. St Ol, starch-oleate; St Pal, starch-palmitate; Suc Ol, sucrose-oleate; Suc Pal, sucrose-palmitate.

significant eWAT necrosis and atrophy over time (Figure 8*A* and *D*), coincident with low levels of DNL and high levels of lipolysis similar to starch-oleate–fed mice (Figure 8*E* and *F*). Finally, adipose tissue from Western diet–fed mice demonstrated an immune profile similar to starch-oleate–fed mice, with elevated numbers of NK, NK^+T^+, and T cells, as well as resident and inflammatory macrophages (Figure 8*G* and *H*). Overall, the comparable outcomes induced by the starch-oleate diet and the Western diet indicate that starch-oleate is sufficient to induce the metabolic derangements of a more complex diet.

Discussion

The experiments in this study underscore that nutrient composition is as important as nutrient content in determining the effect of diet on lipid accumulation in the liver. Using diets with 42% CHO:42% fat, which were designed to mimic the CHO and fat proportions of the average American diet, we found that formulas enriched in monounsaturated fat (oleate) induce more hepatic steatosis than those enriched in saturated fat (palmitate). These data add to the existing literature as many epidemiologic and interventional studies investigating the health effects of dietary fats have tended to focus on comparisons between CHOs and fats, or alternatively between saturated and polyunsaturated, rather than monounsaturated fats.[26,27] Studies that have concentrated specifically on monounsaturated fats have yielded mixed results.[28–30] Our work directly evaluated the health outcomes induced by defined diets differing only in their permutation of CHOs and fats. The data demonstrate that a monounsaturated fat-enriched diet provokes more hepatic steatosis than a saturated fat-enriched diet, particularly when combined with a complex CHO such as starch.

Hepatic lipid derives from 3 major sources: dietary fat, hepatic DNL, and fatty acids released from adipose tissue.[31] The fat content of our high-energy diets was identical, and thus any excess hepatic steatosis induced by the starch-oleate formula should have come from either exaggerated hepatic DNL or increased adipose tissue lipolysis. All 4 high-energy diets stimulated hepatic DNL far beyond that of chow-fed mice, but there was no difference in DNL to distinguish them from each other. Thus, enhanced adipose tissue lipolysis was the likely reason for the disproportionate hepatic lipid accumulation in starch-oleate–fed mice, and this was confirmed experimentally. Oleate-enriched diets have been reported previously to promote adipose tissue lipolysis in rats, but only slightly and only in response to pharmacologic stimulation.[32] In our hands, a starch-oleate diet enhanced basal levels of adipose tissue lipolysis, which over time in vivo led to a significant reduction in adipose tissue mass. Unlike earlier studies in which monounsaturated fat-enriched diets have been shown to slow adipose tissue expansion relative to other high-energy diets,[33] our experiments demonstrated that starch-oleate feeding actually induced progressive necrosis of adipose tissue. The downstream consequence of this adipose tissue involution was worsening of hepatic steatosis.

The initial decline in adipose tissue mass in mice fed the starch-oleate diet was accompanied by evidence of adipose tissue inflammation. The transcriptomic profile of adipose tissue predicted a mixed inflammatory infiltrate comprising NK cells, macrophages, and T lymphocytes, which was confirmed by flow cytometry. The genomic data also documented a decline in several adipocyte-specific differentiation markers; this was consistent with the loss of perilipin by immunohistochemistry. NK cells figured prominently in the adipose tissue infiltrate, which coincides with recent evidence indicating a role for NK cells in the initiation of adipose tissue inflammation in obesity.[34,35] Macrophages and T cells were also increased in numbers in starch-oleate adipose tissue, possibly as a result of recruitment downstream of NK cell activation and infiltration.[34,35] Our experiments did not specifically interrogate for adipose-resident invariant NK T cells, which have been reported to have a unique phenotype.[36,37]

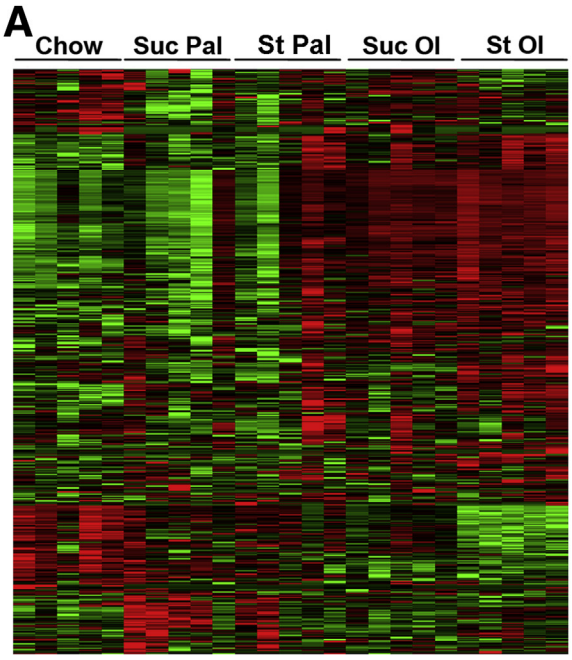

B

Gene Name	vs. Chow	vs. St Pal	vs. Suc Pal	vs. Suc Ol
	Fold Change			
Il12rb2	11.64	2.54	3.25	1.69
Klra8	7.61	2.88	2.77	1.34
Il1a	3.04	7.89	3.12	4.61
Tlr8	2.66	1.65	1.9	1.22
Gzmb	2.37	2.68	2.456	2.21
Tgfb1	1.99	1.63	1.6	1.26
Il17ra	1.47	1.35	1.32	1.25
Cd1d1	-5.55	-2.94	-3.26	-2.6
Icam2	-1.97	-1.55	-1.69	-1.43
Pecam1	-1.72	-1.49	-1.55	-1.52
Pparg	-2.89	-1.84	-1.93	-1.69
Tlr5	-2.87	-2.12	-2.47	-1.45

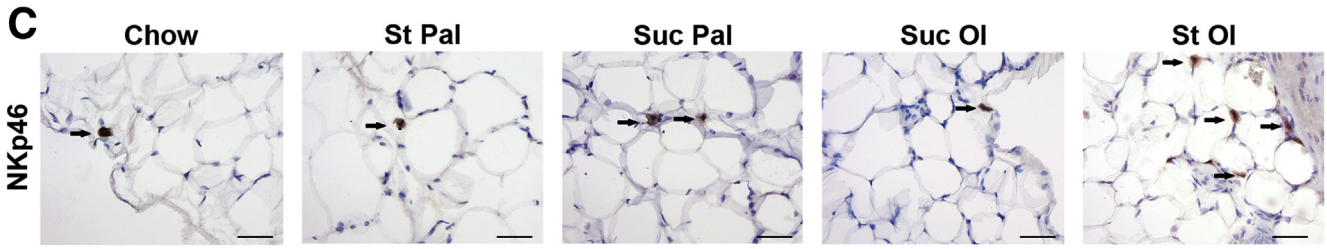

Figure 6. Inflammatory gene expression profile of eWAT in mice fed chow or custom high-energy diets for 6 months. (*A*) Heatmap of eWAT inflammatory gene array organized by diet. (*B*) Select genes for which statistically significant differences in expression were noted between starch-oleate (St Ol) and all other diets. Values represent fold change relative to the indicated comparator group; all values surpassed $P < .05$, for n = 10 performed as replicate experiments of n = 5 each. Complete array data are in Supplementary Table 1. (*C*) eWAT immunohistochemistry for NKp46. Arrows highlight positive cells, which are more abundant in adipose tissue from St Ol–fed mice. Tissue sections were viewed on a Nikon Microphot FXA microscope under a 10× objective and photographed using a Spot camera. Images were compiled in Photoshop CS6 (Adobe Systems Inc, San Jose, CA). Bar = 50 mm. Cd1d1, CD1d molecule; Gzmb, granzyme b; Icam2, intercellular adhesion molecule 2; Il17ra, interleukin 17 receptor a; Il21r, interleukin 21 receptor; Il12rb2, interleukin 12 receptor subunit beta 2; Il1a, interleukin 1a; Klra8, killer cell lectin-like receptor subfamily A, member 8; Pecam1, platelet and endothelial cell adhesion molecule 1; Pparg, peroxisome proliferator activated receptor gamma; St Pal, starch-palmitate; Suc Ol, sucrose-oleate; Suc Pal, sucrose-palmitate; Tgfb1, Transforming growth factor beta 1; Tlr5, Toll-like receptor 5; Tlr8, Toll-like receptor 8.

Why dietary oleate, and especially the combination of starch and oleate, would selectively provoke severe adipose tissue dysfunction is uncertain. Death of adipocytes from oleate accumulation is unlikely, because unsaturated fatty acids are not considered lipotoxic toward these cells.[38,39] Unsaturated fatty acids are also relatively weak activators of macrophages[40–42]; thus, the link between oleate and adipose tissue necrosis and inflammation is likely indirect. Oleate could induce an immune response indirectly in adipose tissue by covalently modifying adipocyte proteins to generate neoantigens.[43,44] Although the mechanism by which oleate damages adipose tissue is currently unknown, studies in humans demonstrate that accumulation of unsaturated fatty acids in adipose tissue is associated with insulin resistance, reduced DNL, and enhanced lipolysis.[45,46] Thus, oleate loading of adipocytes appears to be an important trigger to a decline in adipose tissue mass with resultant hepatic steatosis.

Our observation that a starch-oleate diet induced more hepatic steatosis and adipose tissue dysfunction than did other nutrient combinations is seemingly at odds with other reports that simple sugars and saturated fats have a greater propensity to induce metainflammation and disease.[47,48] In fact, previous studies from our own laboratory have documented the potential for diets containing simple sugars and saturated fats to provoke excess hepatic steatosis and steatohepatitis.[16,49] Notably, our earlier studies combined nutrients in a 60:20 CHO:fat ratio rather than the 42:42 ratio used in the current experiments. Dietary formulas with 60:20 CHO:fat provoke more hepatic DNL than those with

42:42 CHO:fat when compared with chow (A. A. Pierce, 2013 and C. C. Duwaerts, 2014 data not shown). Moreover, in the presence of abundant amounts of simple CHO, even a small amount of dietary saturated fat can accentuate DNL by inducing the enzymes in the lipogenic pathway.[50] The current findings emphasize that the same nutrients, when combined in different proportions, can provoke markedly different effects on the liver and adipose tissue.

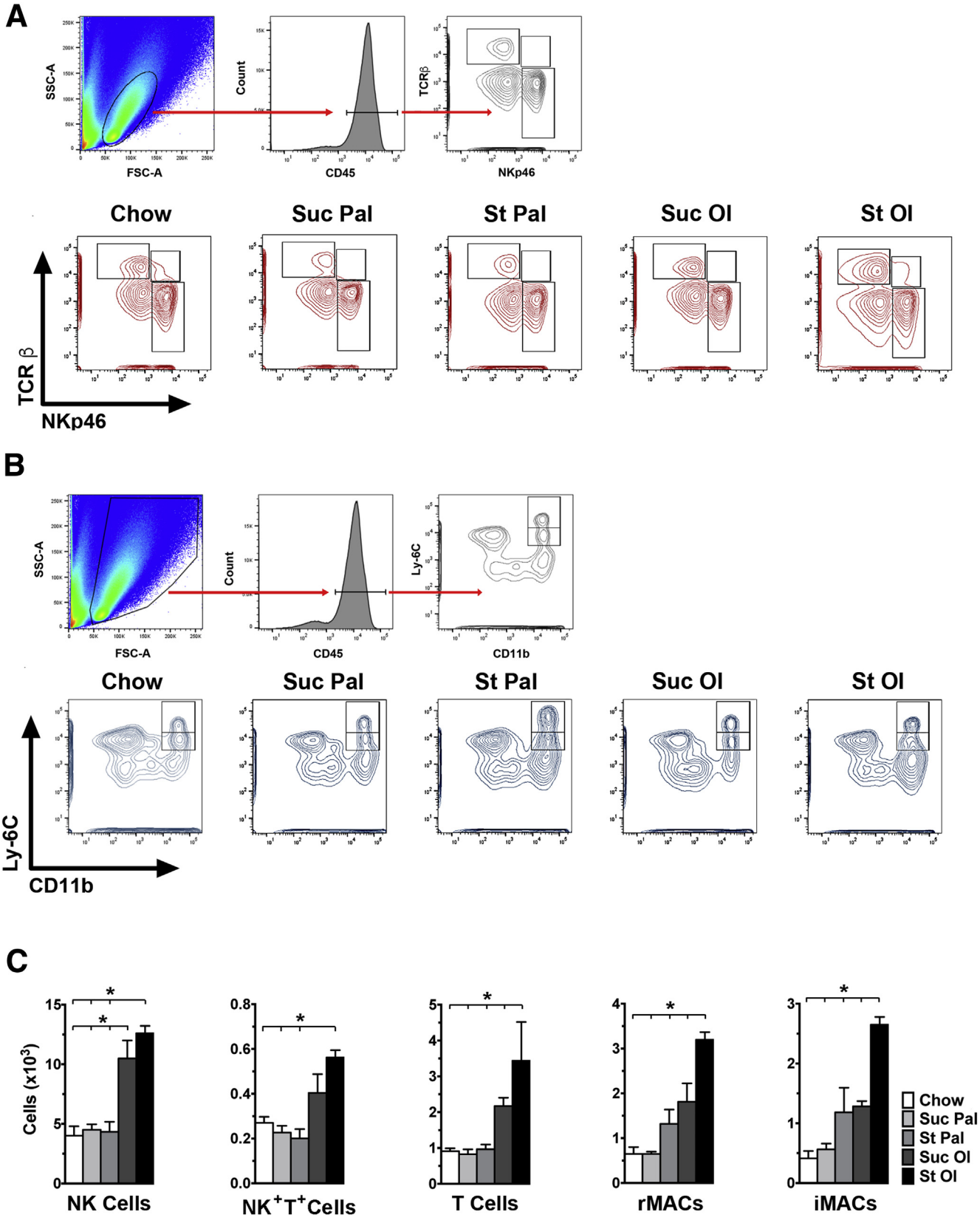

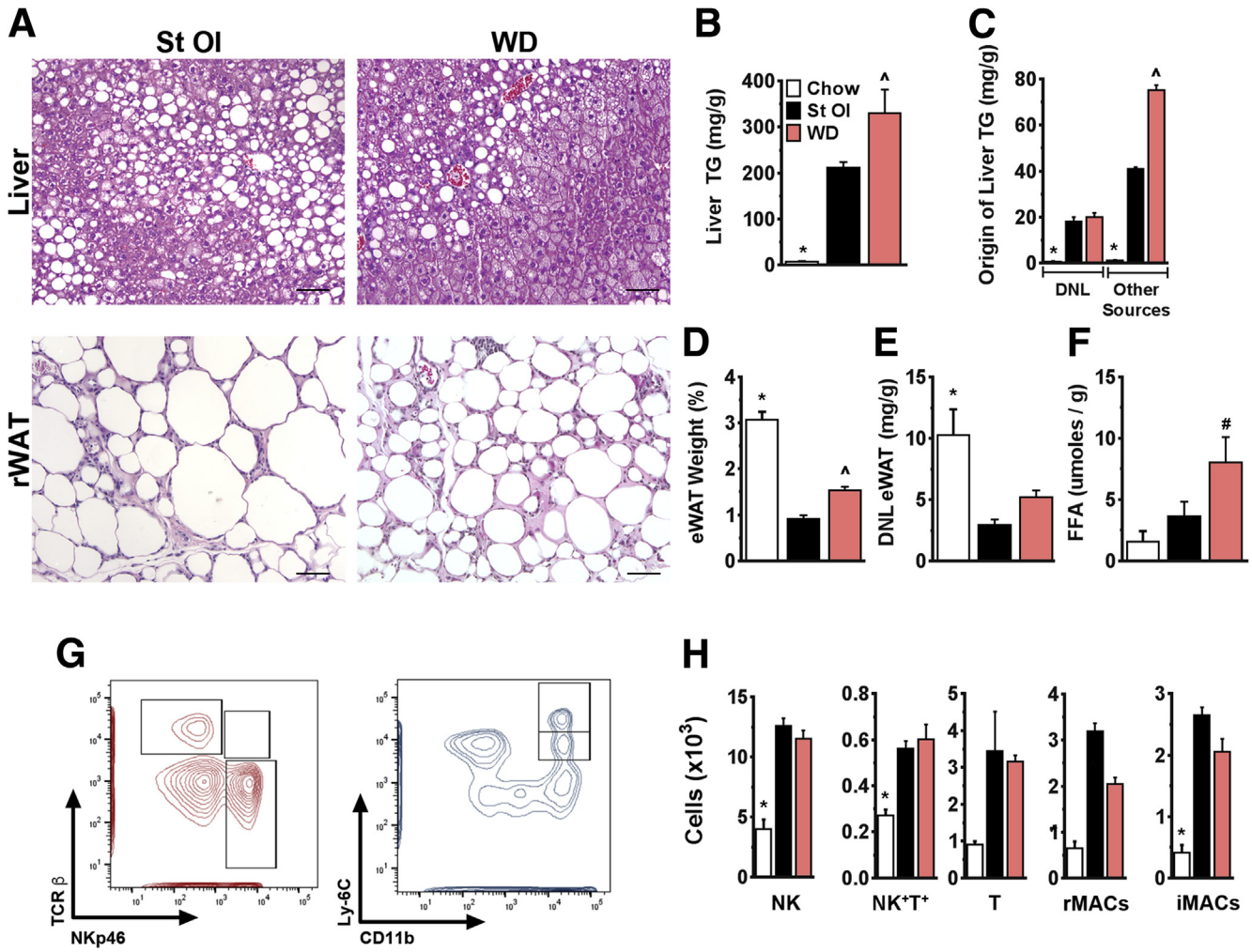

Figure 8. Features of mice fed WD, St Ol, and chow for 6 months. Data for starch-oleate (St Ol) and chow mice are reproduced from Figures 2 to 5 and Figure 7. (*A*) Photomicrographs of H&E-stained liver and eWAT. Bar = 100 μm. (*B*) Liver TG content. (*C*) Hepatic lipid (palmitate) originating from DNL or other sources. (*D*) eWAT weight as a percent of total body weight. (*E*) Adipose tissue DNL. (*F*) Adipose tissue lipolysis ex vivo. (*G*) Contour plots distinguishing NK cells (NKp46$^+$,TCRβ^-), NK$^+$T$^+$ cells (NKp46$^+$, TCRβ^+), and T cells (NKp46$^-$, TCRβ^+) as well as resident macrophages (CD11b$^+$, Ly6C^{int}) and infiltrating macrophages (CD11b$^+$, Ly6C^{hi}) in eWAT from mice fed a Western diet (WD). (*H*) Absolute cell numbers of each cell population based on flow cytometry data. Values represent mean ± SE for n = 10, performed as replicate experiments of n=5 each. $^*P < .05$ to all other groups, $^\#P < .05$ to chow, $^\wedge P < .05$ to St Ol. FFA, free fatty acids; iMACs, infiltrating macrophages; rMACs, resident macrophages; TCRβ, T-cell receptor beta.

The diets used in this study were rigorously defined with a limited number of macronutrients to facilitate the assessment of individual nutrient effects on liver and adipose tissue. These custom diets have limitations in that they do not faithfully represent the complex nutrient composition of the human diet. Still, despite its restricted composition, the starch-oleate diet produced nearly identical metabolic effects on mice fed as a mixed-nutrient "Western diet" over a 6-month interval. Although the Western diet is more nutrient diverse than the starch-oleate diet is, the 2 formulas have similar caloric densities and similar proportions of CHO and fat. The fact that starch-

Figure 7. (*See previous page*). Immunophenotyping of eWAT in mice fed chow or custom high-energy diets for 6 weeks. Stromal vascular cells from adipose tissue were analyzed by flow cytometry after initial gating on CD45$^+$ lymphocytes (*A*) or CD45$^+$ live cells (*B*). (*A*) *Top panel*: gating strategy for this population. *Bottom panel*: contour plots distinguishing NK cells (NKp46$^+$,TCRb$^-$), NK$^+$T$^+$ cells (NKp46$^+$, TCRb$^+$), and T cells (NKp46$^-$, TCRb$^+$) in eWAT. (*B*) *Top panel*: gating strategy for this population. *Bottom panel*: flow cytometry plots distinguishing resident macrophages (CD11b$^+$, Ly6C^{int}) from infiltrating macrophages (CD11b$^+$, Ly6C^{hi}) in eWAT. (*C*) Absolute cell numbers of each cell population based on flow cytometry data. Values represent mean ± SE for n = 5 mice. $^*P < .05$. CD45, cluster of differentiation 45; FSC-A, forward scatter-area; iMACs, infiltrating macrophages; rMACs, resident macrophages; SSC-A, side scatter-area; St Ol, starch-oleate; St Pal, starch-palmitate; Suc Ol, sucrose-oleate; Suc Pal, sucrose-palmitate; TCRβ, T-cell receptor beta.

oleate phenocopied the effect of the Western diet in mice provides a strong rationale to further pursue the disease-promoting potential of this nutrient pair.

The data in this study were generated with C3H mice rather than the more commonly used C57BL/6 strain. We used C3H/HeOuJ mice, which, unlike the mutant substrain C3H/HeJ, exhibit normal Toll-like receptor signaling. We found in preliminary experiments that C3H/HeOuJ mice exhibited more rapid hepatic steatosis and adipose tissue involution than C57BL/6J mice did. Interstrain differences in dietary responses are known to occur[51–53] and provide additional opportunity for exploration.

In summary, the current study demonstrates that a diet balanced in CHO and fat but highly enriched in monounsaturated fat can produce pronounced dysfunction of visceral adipose tissue, resulting in hepatic steatosis. This corroborates observations in humans, in which excess accumulation of oleate in adipose tissue coincides with insulin resistance. Although dietary oleate has been purported to have many health benefits including a favorable circulating lipid profile,[54] too much monounsaturated fat in the diet can have significant adverse effects on metabolism. This discovery calls for close examination of the detrimental effects of dietary oleate, as well as further efforts to determine the appropriate balance of nutrient content and composition to foster metabolic homeostasis.

References

1. Flegal KM, Kruszon-Moran D, Carroll MD, Fryar CD, Ogden CL. Trends in obesity among adults in the United States, 2005 to 2014. JAMA 2016;315:2284–2291.
2. Ng M, Fleming T, Robinson M, Thomson B, Graetz N, Margono C, Mullany EC, Biryukov S, Abbafati C, Abera SF, Abraham JP, Abu-Rmeileh NM, Achoki T, AlBuhairan FS, Alemu ZA, Alfonso R, Ali MK, Ali R, Guzman NA, Ammar W, Anwari P, Banerjee A, Barquera S, Basu S, Bennett DA, Bhutta Z, Blore J, Cabral N, Nonato IC, Chang JC, Chowdhury R, Courville KJ, Criqui MH, Cundiff DK, Dabhadkar KC, Dandona L, Davis A, Dayama A, Dharmaratne SD, Ding EL, Durrani AM, Esteghamati A, Farzadfar F, Fay DF, Feigin VL, Flaxman A, Forouzanfar MH, Goto A, Green MA, Gupta R, Hafezi-Nejad N, Hankey GJ, Harewood HC, Havmoeller R, Hay S, Hernandez L, Husseini A, Idrisov BT, Ikeda N, Islami F, Jahangir E, Jassal SK, Jee SH, Jeffreys M, Jonas JB, Kabagambe EK, Khalifa SE, Kengne AP, Khader YS, Khang YH, Kim D, Kimokoti RW, Kinge JM, Kokubo Y, Kosen S, Kwan G, Lai T, Leinsalu M, Li Y, Liang X, Liu S, Logroscino G, Lotufo PA, Lu Y, Ma J, Mainoo NK, Mensah GA, Merriman TR, Mokdad AH, Moschandreas J, Naghavi M, Naheed A, Nand D, Narayan KM, Nelson EL, Neuhouser ML, Nisar MI, Ohkubo T, Oti SO, Pedroza A, Prabhakaran D, Roy N, Sampson U, Seo H, Sepanlou SG, Shibuya K, Shiri R, Shiue I, Singh GM, Singh JA, Skirbekk V, Stapelberg NJ, Sturua L, Sykes BL, Tobias M, Tran BX, Trasande L, Toyoshima H, van de Vijver S, Vasankari TJ, Veerman JL, Velasquez-Melendez G, Vlassov VV, Vollset SE, Vos T, Wang C, Wang X, Weiderpass E, Werdecker A, Wright JL, Yang YC, Yatsuya H, Yoon J, Yoon SJ, Zhao Y, Zhou M, Zhu S, Lopez AD, Murray CJ, Gakidou E. Global, regional, and national prevalence of overweight and obesity in children and adults during 1980–2013: a systematic analysis for the Global Burden of Disease Study 2013. Lancet 2014;384:766–781.
3. Rey-Lopez JP, de Rezende LF, Pastor-Valero M, Tess BH. The prevalence of metabolically healthy obesity: a systematic review and critical evaluation of the definitions used. Obes Rev 2014;15:781–790.
4. Samocha-Bonet D, Dixit VD, Kahn CR, Leibel RL, Lin X, Nieuwdorp M, Pietilainen KH, Rabasa-Lhoret R, Roden M, Scherer PE, Klein S, Ravussin E. Metabolically healthy and unhealthy obese–the 2013 Stock Conference report. Obes Rev 2014;15:697–708.
5. Chang Y, Jung HS, Cho J, Zhang Y, Yun KE, Lazo M, Pastor-Barriuso R, Ahn J, Kim CW, Rampal S, Cainzos-Achirica M, Zhao D, Chung EC, Shin H, Guallar E, Ryu S. Metabolically healthy obesity and the development of nonalcoholic fatty liver disease. Am J Gastroenterol 2016;111:1133–1140.
6. Green AK, Jacques PF, Rogers G, Fox CS, Meigs JB, McKeown NM. Sugar-sweetened beverages and prevalence of the metabolically abnormal phenotype in the Framingham Heart Study. Obesity 2014;22:E157–E163.
7. Camhi SM, Whitney Evans E, Hayman LL, Lichtenstein AH, Must A. Healthy eating index and metabolically healthy obesity in U.S. adolescents and adults. Prev Med 2015;77:23–27.
8. Phillips CM, Dillon C, Harrington JM, McCarthy VJ, Kearney PM, Fitzgerald AP, Perry IJ. Defining metabolically healthy obesity: role of dietary and lifestyle factors. PLoS One 2013;8:e76188.
9. Fung MD, Canning KL, Mirdamadi P, Ardern CI, Kuk JL. Lifestyle and weight predictors of a healthy overweight profile over a 20-year follow-up. Obesity 2015;23:1320–1325.
10. Kimokoti RW, Judd SE, Shikany JM, Newby PK. Metabolically healthy obesity is not associated with food intake in white or black men. J Nutr 2015;145:2551–2561.
11. Kirk E, Reeds DN, Finck BN, Mayurranjan SM, Patterson BW, Klein S. Dietary fat and carbohydrates differentially alter insulin sensitivity during caloric restriction. Gastroenterology 2009;136:1552–1560.
12. Stanhope KL, Schwarz JM, Keim NL, Griffen SC, Bremer AA, Graham JL, Hatcher B, Cox CL, Dyachenko A, Zhang W, McGahan JP, Seibert A, Krauss RM, Chiu S, Schaefer EJ, Ai M, Otokozawa S, Nakajima K, Nakano T, Beysen C, Hellerstein MK, Berglund L, Havel PJ. Consuming fructose-sweetened, not glucose-sweetened, beverages increases visceral adiposity and lipids and decreases insulin sensitivity in overweight/obese humans. J Clin Invest 2009;119:1322–1334.
13. Rosqvist F, Iggman D, Kullberg J, Cedernaes J, Johansson HE, Larsson A, Johansson L, Ahlstrom H, Arner P, Dahlman I, Riserus U. Overfeeding polyunsaturated and saturated fat causes distinct effects on

liver and visceral fat accumulation in humans. Diabetes 2014;63:2356–2368.
14. Chiu S, Sievenpiper JL, de Souza RJ, Cozma AI, Mirrahimi A, Carleton AJ, Ha V, Di Buono M, Jenkins AL, Leiter LA, Wolever TM, Don-Wauchope AC, Beyene J, Kendall CW, Jenkins DJ. Effect of fructose on markers of non-alcoholic fatty liver disease (NAFLD): a systematic review and meta-analysis of controlled feeding trials. Eur J Clin Nutr 2014;68:416–423.
15. Teng KT, Chang LF, Vethakkan SR, Nesaretnam K, Sanders TA. Effects of exchanging carbohydrate or monounsaturated fat with saturated fat on inflammatory and thrombogenic responses in subjects with abdominal obesity: a randomized controlled trial. Clin Nutr 2016 Sep 8, pii: S0261-5614(16)30236-9.
16. Pierce AA, Duwaerts CC, Soon RK, Siao K, Grenert JP, Fitch M, Hellerstein MK, Beysen C, Turner SM, Maher JJ. Isocaloric manipulation of macronutrients within a high-carbohydrate/moderate-fat diet induces unique effects on hepatic lipogenesis, steatosis and liver injury. J Nutr Biochem 2016;29:12–20.
17. Folch J, Lees M, Sloane Stanley GH. A simple method for the isolation and purification of total lipides from animal tissues. J Biol Chem 1957;226:497–509.
18. Pickens MK, Yan JS, Ng RK, Ogata H, Grenert JP, Beyson C, Turner SM, Maher JJ. Dietary sucrose is essential to the development of liver injury in the MCD model of steatohepatitis. J Lipid Res 2009;50:2072–2082.
19. Kleiner DE, Brunt EM, Van Natta M, Behling C, Contos MJ, Cummings OW, Ferrell LD, Liu YC, Torbenson MS, Unalp-Arida A, Yeh M, McCullough AJ, Sanyal AJ. Design and validation of a histological scoring system for nonalcoholic fatty liver disease. Hepatology 2005;41:1313–1321.
20. Segura S, Requena L. Anatomy and histology of normal subcutaneous fat, necrosis of adipocytes, and classification of the panniculitides. Dermatol Clin 2008;26:419–424, v.
21. Jones PJ. Tracing lipogenesis in humans using deuterated water. Can J Physiol Pharmacol 1996;74:755–760.
22. Hellerstein MK, Neese RA. Mass isotopomer distribution analysis at eight years: theoretical, analytic, and experimental considerations. Am J Physiol 1999; 276:E1146–E1170.
23. Turner SM, Roy S, Sul HS, Neese RA, Murphy EJ, Samandi W, Roohk DJ, Hellerstein MK. Dissociation between adipose tissue fluxes and lipogenic gene expression in ob/ob mice. Am J Physiol Endocrinol Metab 2007;292:E1101–E1109.
24. Cinti S, Mitchell G, Barbatelli G, Murano I, Ceresi E, Faloia E, Wang S, Fortier M, Greenberg AS, Obin MS. Adipocyte death defines macrophage localization and function in adipose tissue of obese mice and humans. J Lipid Res 2005;46:2347–2355.
25. Bezman NA, Kim CC, Sun JC, Min-Oo G, Hendricks DW, Kamimura Y, Best JA, Goldrath AW, Lanier LL. Molecular definition of the identity and activation of natural killer cells. Nat Immunol 2012;13:1000–1009.
26. Siri-Tarino PW, Sun Q, Hu FB, Krauss RM. Saturated fat, carbohydrate, and cardiovascular disease. Am J Clin Nutr 2010;91:502–509.
27. Schwingshackl L, Hoffmann G. Monounsaturated fatty acids and risk of cardiovascular disease: synopsis of the evidence available from systematic reviews and meta-analyses. Nutrients 2012;4:1989–2007.
28. Kouvari M, Notara V, Panagiotakos DB, Michalopoulou M, Vassileiou N, Papataxiarchis E, Tzanoglou D, Mantas Y, Kogias Y, Stravopodis P, Papanagnou G, Zombolos S, Pitsavos C. Exclusive olive oil consumption and 10-year (2004–2014) acute coronary syndrome incidence among cardiac patients: the GREECS observational study. J Hum Nutr Diet 2016; 29:354–362.
29. Jebb SA, Lovegrove JA, Griffin BA, Frost GS, Moore CS, Chatfield MD, Bluck LJ, Williams CM, Sanders TA. Effect of changing the amount and type of fat and carbohydrate on insulin sensitivity and cardiovascular risk: the RISCK (Reading, Imperial, Surrey, Cambridge, and Kings) trial. Am J Clin Nutr 2010;92:748–758.
30. Miller M, Sorkin JD, Mastella L, Sutherland A, Rhyne J, Donnelly P, Simpson K, Goldberg AP. Poly is more effective than monounsaturated fat for dietary management in the metabolic syndrome: the muffin study. J Clin Lipidol 2016;10:996–1003.
31. Donnelly KL, Smith CI, Schwarzenberg SJ, Jessurun J, Boldt MD, Parks EJ. Sources of fatty acids stored in liver and secreted via lipoproteins in patients with nonalcoholic fatty liver disease. J Clin Invest 2005; 115:1343–1351.
32. Garcia-Escobar E, Soriguer F, Garcia-Serrano S, Gomez-Zumaquero JM, Morcillo S, Haro J, Rojo-Martinez G. Dietary oleic acid and adipocyte lipolytic activity in culture. J Nutr Biochem 2008;19:727–731.
33. Hsu SC, Huang CJ. Reduced fat mass in rats fed a high oleic acid-rich safflower oil diet is associated with changes in expression of hepatic PPARalpha and adipose SREBP-1c-regulated genes. J Nutr 2006; 136:1779–1785.
34. Wensveen FM, Jelencic V, Valentic S, Sestan M, Wensveen TT, Theurich S, Glasner A, Mendrila D, Stimac D, Wunderlich FT, Bruning JC, Mandelboim O, Polic B. NK cells link obesity-induced adipose stress to inflammation and insulin resistance. Nat Immunol 2015; 16:376–385.
35. Lee BC, Kim MS, Pae M, Yamamoto Y, Eberle D, Shimada T, Kamei N, Park HS, Sasorith S, Woo JR, You J, Mosher W, Brady HJ, Shoelson SE, Lee J. Adipose natural killer cells regulate adipose tissue macrophages to promote insulin resistance in obesity. Cell Metabolism 2016;23:685–698.
36. Lynch L, Michelet X, Zhang S, Brennan PJ, Moseman A, Lester C, Besra G, Vomhof-Dekrey EE, Tighe M, Koay HF, Godfrey DI, Leadbetter EA, Sant'Angelo DB, von Andrian U, Brenner MB. Regulatory iNKT cells lack expression of the transcription factor PLZF and control the homeostasis of T(reg) cells and macrophages in adipose tissue. Nat Immunol 2015;16:85–95.
37. Vieth JA, Das J, Ranaivoson FM, Comoletti D, Denzin LK, Sant'Angelo DB. TCRalpha-TCRbeta pairing controls recognition of CD1d and directs the development of adipose NKT cells. Nat Immunol 2017;18:36–44.

38. Lundgren M, Eriksson JW. No in vitro effects of fatty acids on glucose uptake, lipolysis or insulin signaling in rat adipocytes. Horm Metab Res 2004;36:203–209.
39. Guo W, Wong S, Xie W, Lei T, Luo Z. Palmitate modulates intracellular signaling, induces endoplasmic reticulum stress, and causes apoptosis in mouse 3T3-L1 and rat primary preadipocytes. Am J Physiol Endocrinol Metab 2007;293:E576–E586.
40. Lee JY, Sohn KH, Rhee SH, Hwang D. Saturated fatty acids, but not unsaturated fatty acids, induce the expression of cyclooxygenase-2 mediated through Toll-like receptor 4. J Biol Chem 2001;276:16683–16689.
41. Wen H, Gris D, Lei Y, Jha S, Zhang L, Huang MT, Brickey WJ, Ting JP. Fatty acid-induced NLRP3-ASC inflammasome activation interferes with insulin signaling. Nat Immunol 2011;12:408–415.
42. Pardo V, Gonzalez-Rodriguez A, Guijas C, Balsinde J, Valverde AM. Opposite cross-talk by oleate and palmitate on insulin signaling in hepatocytes through macrophage activation. J Biol Chem 2015;290:11663–11677.
43. Maris M, Waelkens E, Cnop M, D'Hertog W, Cunha DA, Korf H, Koike T, Overbergh L, Mathieu C. Oleate-induced beta cell dysfunction and apoptosis: a proteomic approach to glucolipotoxicity by an unsaturated fatty acid. J Proteome Res 2011;10:3372–3385.
44. Klein-Wieringa IR, Andersen SN, Kwekkeboom JC, Giera M, de Lange-Brokaar BJ, van Osch GJ, Zuurmond AM, Stojanovic-Susulic V, Nelissen RG, Pijl H, Huizinga TW, Kloppenburg M, Toes RE, Ioan-Facsinay A. Adipocytes modulate the phenotype of human macrophages through secreted lipids. J Immunol 2013;191:1356–1363.
45. Yew Tan C, Virtue S, Murfitt S, Roberts LD, Phua YH, Dale M, Griffin JL, Tinahones F, Scherer PE, Vidal-Puig A. Adipose tissue fatty acid chain length and mono-unsaturation increases with obesity and insulin resistance. Sci Rep 2015;5:18366.
46. Allister CA, Liu LF, Lamendola CA, Craig CM, Cushman SW, Hellerstein MK, McLaughlin TL. In vivo 2H2O administration reveals impaired triglyceride storage in adipose tissue of insulin-resistant humans. J Lipid Res 2015;56:435–439.
47. Sobrecases H, Le KA, Bortolotti M, Schneiter P, Ith M, Kreis R, Boesch C, Tappy L. Effects of short-term overfeeding with fructose, fat and fructose plus fat on plasma and hepatic lipids in healthy men. Diabetes Metab 2010; 36:244–246.
48. Tetri LH, Basaranoglu M, Brunt EM, Yerian LM, Neuschwander-Tetri BA. Severe NAFLD with hepatic necroinflammatory changes in mice fed trans fats and a high-fructose corn syrup equivalent. Am J Physiol Gastrointest Liver Physiol 2008;295:G987–G995.
49. Pierce AA, Pickens MK, Siao K, Grenert JP, Maher JJ. Differential hepatotoxicity of dietary and DNL-derived palmitate in the methionine-choline-deficient model of steatohepatitis. BMC Gastroenterol 2015;15:72.
50. Lin J, Yang R, Tarr PT, Wu PH, Handschin C, Li S, Yang W, Pei L, Uldry M, Tontonoz P, Newgard CB, Spiegelman BM. Hyperlipidemic effects of dietary saturated fats mediated through PGC-1beta coactivation of SREBP. Cell 2005;120:261–273.
51. Rangnekar AS, Lammert F, Igolnikov A, Green RM. Quantitative trait loci analysis of mice administered the methionine-choline deficient dietary model of experimental steatohepatitis. Liver Int 2006; 26:1000–1005.
52. Fengler VH, Macheiner T, Kessler SM, Czepukojc B, Gemperlein K, Muller R, Kiemer AK, Magnes C, Haybaeck J, Lackner C, Sargsyan K. Susceptibility of different mouse wild type strains to develop diet-induced NAFLD/AFLD-associated liver disease. PLoS One 2016; 11:e0155163.
53. Asgharpour A, Cazanave SC, Pacana T, Seneshaw M, Vincent R, Banini BA, Kumar DP, Daita K, Min HK, Mirshahi F, Bedossa P, Sun X, Hoshida Y, Koduru SV, Contaifer D Jr, Warncke UO, Wijesinghe DS, Sanyal AJ. A diet-induced animal model of non-alcoholic fatty liver disease and hepatocellular cancer. Journal of hepatology 2016;65:579–588.
54. Kris-Etherton PM. AHA Science Advisory. Monounsaturated fatty acids and risk of cardiovascular disease. American Heart Association. Nutrition Committee. Circulation 1999;100:1253–1258.

Received January 19, 2017. Accepted April 12, 2017.

Correspondence
Address correspondence to: Jacquelyn J. Maher, MD, Liver Center Laboratory, 1001 Potrero Avenue, Building 40, Room 4102, San Francisco, California 94110. e-mail: jacquelyn.maher@ucsf.edu; fax: (415) 641-0517.

Acknowledgments
The authors are grateful to Dr Andrew Pierce for assistance with adipose tissue collection, Dr Marc Hellerstein for helpful discussions about adipose tissue lipid homeostasis, and the Mouse Metabolic Phenotyping Core at Vanderbilt University for performing fatty acid analysis on liver tissue (U24 DK059637).

Author contributions
Study design (CCD, JJM); data acquisition (CCD, AMA, KS, CH, CB, MF, AG, JPG, SJC); data analysis and interpretation (CCD, AMA, CB, MF, AG, JB, JJM); manuscript preparation (CCD, JJM); and critical revision of manuscript (JLB).

Conflicts of interest
The authors declare no conflicts.

Funding
This study was supported by R01 DK068450 (J.J.M.), T32 DK068414 (C.C.D., A.M.A.), the UCSF Liver Center (P30 DK026743), and the Vanderbilt Mouse Metabolic Phenotyping Center (U24 DK059637).